

NCAM: Near-Data Processing for Nearest Neighbor Search

Vincent T. Lee, Carlo C. del Mundo, Armin Alaghi, Luis Ceze, Mark Oskin, Ali Farhadi
University of Washington
{vlee2, cdel, armin, luisceze, oskin, ali}@cs.washington.edu

ABSTRACT

Deep down in many applications like natural language processing (NLP), vision, and robotics is a form of the k-nearest neighbor search algorithm (kNN). The kNN algorithm is primarily bottlenecked by data movement, limiting throughput and incurring latency in these applications. While there do exist well bounded kNN approximations that improve the performance of kNN, these algorithms trade-off accuracy and quickly degrade into linear search for high dimensionality.

To address data movement, we designed the nearest neighbor content addressable memory (NCAM) which employs processing in-memory (PIM) to eliminate costly data transfers, and provides exact nearest neighbor search. NCAMs benefit from the modularity offered by 3D die-stacking technology which allows us to side-step the issues of direct integration with DRAM dies. The NCAM benefits from the higher density and speeds of emerging memory technologies and interfaces.

We characterize a state-of-the-art software kNN implementation and expose the shortcomings of approximate kNN search. We present a full NCAM design and estimate its performance using post-placement and route estimates, and we show that its power characteristics are compatible with emerging memory substrates. We then evaluate energy efficiency and latency compared to modern multi-core CPUs and GPGPU platforms using parameters typical of mobile and server workloads. Our simulation results show that the NCAM can achieve up to $160\times$ throughput per watt and three orders of magnitude latency improvement over a NVIDIA Titan X GPU for server workloads, and $\sim 2413\times$ throughput per watt and $\sim 94.5\times$ latency improvements over a multi-core Intel E5-2620 CPU. Finally, we show that the NCAM is not limited to just kNN and can be generalized to act as a content addressable memory (CAM) or ternary-CAM (TCAM).

1. INTRODUCTION

The growth of media content combined with advances in NLP, vision, and robotics have proliferated a number of applications such as document retrieval [1, 2], content-based search [3], and motion planning [4]. A fundamental primitive to each of these applications is

a similarity search for a given query. The query is typically a *feature vector* which is an intermediate representation of raw media. Feature vectors may represent the trajectories of pixels in a video, word embedding from a corpus of documents, or shapes in an image. For many applications, it is necessary to find some set of similar feature vectors provided in a dataset where similarity is defined by a distance metric such as Hamming or Euclidean distance. The problem of computing the distances between a query feature vector and a dataset of candidates is known as k-nearest neighbors (kNN).

Solutions such as general purpose GPUs (GPGPUs) and multi-core CPUs are memory starved. While individual distance calculations are cheap and highly parallelizable across the dataset, moving feature vector data from memory to the compute device is a huge bottleneck. Moreover, this data is used only once per kNN query and discarded; the result of a kNN query is only a handful of identifiers. Many uses of kNN depend on query *throughput*, and hence a common strategy is to process many queries at once, amortizing this data movement cost. On the other hand, interactive applications demand low latency. Performance is further exacerbated by the *curse of dimensionality* [5] and is amplified by the exponential growth in media content. While approximate variants of kNN can improve search time by pruning the search space using preprocessed data structures, these algorithms result in undesirable losses in accuracy. Furthermore, prior works have shown that with higher dimensionality, these hierarchical data structures like kd-trees and k-means clustering tend to degrade to linear search [6–8].

Because of its significance, generality, parallelism, underlying simplicity, and small result set, kNN is a good candidate for acceleration with logic in the memory system itself. The key insight is that a relatively small compute engine for kNN is compatible with memory module power budgets, and can apply orders of magnitude data reduction, substantially reducing the need for data movement. While there have been many attempts at processing in memory (PIM) in the past [9–14], much of prior work suffered from DRAM technological limitations. Logic created in DRAM processes was too slow, while DRAM implemented in logic processes suffered from poor retention and high power demands; attempts at hybrid processes [15] resulted in the worst of both.

PIM architectures are more viable today with the advent of die stacking technology which enables the co-existence of an efficient DRAM layer *and* an efficient logic layer [16].

We propose the Nearest Neighbor Content Addressable Memory (NCAM) which integrates a programmable accelerator with die-stacked DRAM. Semantically, the NCAM takes a query vector as input, and returns the top-k closest neighbors stored in memory as output by performing parallelized linear search. We demonstrate the efficacy of the NCAM by designing, synthesizing, and simulating the device. Our paper makes the following contributions:

- **Characterization.** We characterize k-nearest neighbors, and we demonstrate the shortcomings of state-of-the-art software implementations.
- **Architecture/Design.** We design the nearest neighbor content addressable memory in the context of emerging memory technologies such as the Hybrid Memory Cube [16].
- **Evaluation.** We evaluate the NCAM’s throughput and latency against a multi-core CPU, a Titan X GPU, and an embedded Tegra K1 SoC. We show that the NCAM improves energy efficiency by 2-4 orders of magnitude against these platforms.

We describe and characterize kNN in Section 2. Section 3 describes the microarchitecture of the NCAM. Section 4 describes the hardware/software interface. Section 5 describes our methodology to evaluate the NCAM design. Section 6 evaluates the NCAM and compares it to commercially available alternatives. Section 7 discusses the impact of these results on different application areas and design points. In Section 8, we discuss past related efforts. We conclude in Section 9.

2. CHARACTERIZATION

We use content-based search [3] as an example application where kNN performance is vitally important. In this section we present the software pipeline for content-based search (Figure 1) and contemporary solutions to kNN. We then highlight the shortcomings and identify the bottlenecks for kNN, and show that state-of-the-art approximate algorithms for kNN degrade to linear search. Finally, we outline typical application design points for our exploration going forward.

2.1 Example Application: Content-Based Search

Figure 1 shows the software pipeline for content-based search. We describe each piece of this pipeline below:

Feature extraction (Figure 1a): Content-based search requires pre-processing of the media into a discriminative intermediate feature vector representation. In our characterization, we extracted features from images using the AlexNet neural network implemented in the Berkeley Caffe framework [17]. Although feature extraction is an important component of this pipeline, a

significant body of prior work has already demonstrated features extraction can be achieved efficiently [18–22].

Indexing (Figure 1b): In state-of-the-art kNN implementations, data structures such as kd-trees or k-means clustering are employed. At query time, these data structures are used to quickly prune the search space; intuitively these data structures should be able to reduce the search time from linear to logarithmic. However, we corroborate past results that show this is not the case in practice [6–8].

Query generation (Figure 1c): While feature extraction and indexing can be performed offline, this phase of the pipeline occurs online when a user may input a query media file (an image, video, etc.) and request similar media content back. The input query is run through the same feature extractor used to create the database before being sent to the search phase.

k-nearest neighbors (Figure 1d): Using the feature representation of the query, this phase performs the search by comparing the query vector against a database for similar content. Many different distance metrics of similarity exist. For our characterization, we choose two proven metrics: Euclidean and Hamming. While Euclidean is the canonical distance metric, Hamming distance has also been shown to achieve excellent results [23–28].

Reverse lookup (Figure 1e): The final step is to take the resulting k nearest neighbors and reverse lookup the content in the database. The result media is then returned to the user.

2.2 Software and algorithm characterization of kNN

The primary problem of kNN search is the *curse of dimensionality* [5]. To ameliorate the issue of dimensionality, the search is approximated using indexing data structures [5, 8, 29] where accuracy is sacrificed for better execution time. In approximate nearest neighbors, the search may not find the exact closest neighbors. The approximate search maintains a priority queue of *most likely* closest branches and investigates branches starting with the most promising candidates. Increasing search time increases the level of accuracy as the algorithm is given more time to traverse branches in the data structure. A time out constraint specifies when the algorithm should give up in the search and return its best found matches. However, even these approximation techniques are not immune to the curse of dimensionality and prior works have indicated hierarchical indexing algorithms like kd-trees and k-means clusters — which are supposed to improve search time by pruning the space — *degrades to brute-force linear search* [6–8].

To evaluate the efficacy of approximation and to further guide our design space exploration, we benchmarked the Fast Library for Approximate Nearest Neighbors (FLANN) [29], a widely used kNN library. We used images from the Yahoo! Flickr dataset [30] and extracted features using AlexNet. We benchmarked FLANN’s three search strategies: linear search, parallel randomized kd-trees, and priority search k-means.

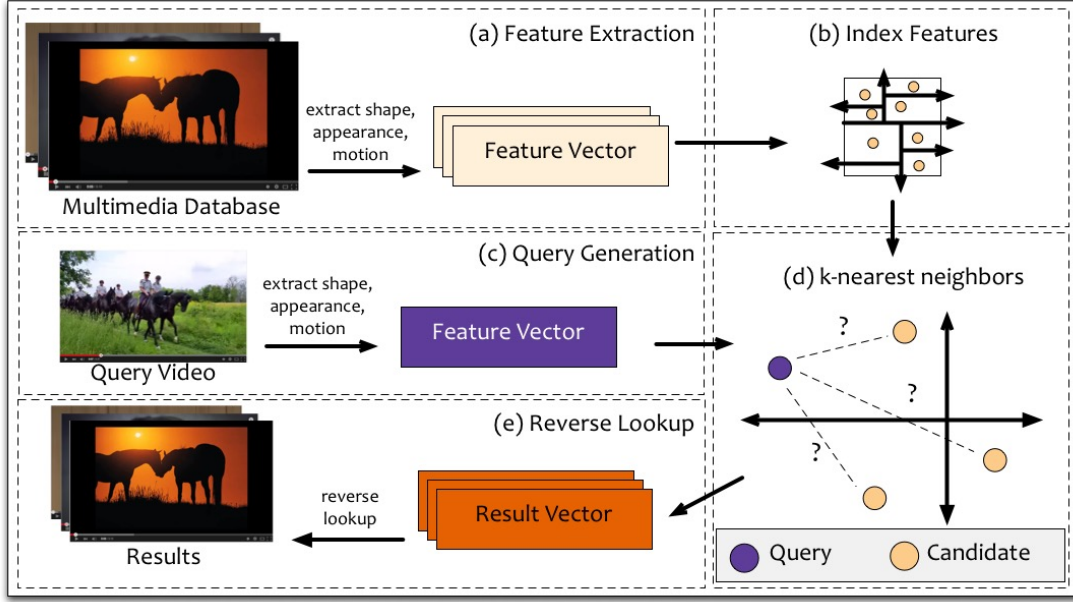


Figure 1: Content based search pipeline: Features are extracted from media content and stored in a dataset (a). To find similar content the same features are extracted from the query (c). The dataset (d) is searched for the k-nearest neighbors, possibly using an index (b). Finally the resulting media is returned to the user (e). The relevant stages that this work addresses are (b) and (d).

Linear search: This search strategy requires no data structure. It is exact (i.e. no approximation) and searches by scanning through the dataset. A distance calculation is performed for every query-candidate pair, and results are stored in a priority queue. The algorithm’s complexity is $O(Q \times N)$ where Q is the number of query vectors and N is the number of data vectors in the dataset. Linear search is accurate, but is slow and is considered the worst-case upper bound for searching.

Parallel randomized kd-trees: This approach approximates nearest neighbor search by constructing and searching multiple kd-trees in parallel. In each kd-tree, cuts are selected by randomly selecting the top- N (we use $N = 4$) most varying dimensions. Each tree, when built, has a different permutation of hyper plane cuts. During search, a priority queue is maintained and is shared across all trees keeping track of already visited branches. We will refer to the parallel randomized kd-trees approach simply as **kd-tree**.

Priority search k-means: In this approach, a priority queue and a k-means data structure is used to approximate kNN. The hierarchical data structure is constructed by initially clustering the dataset into k clusters using the k-means algorithm. Vectors in the same cluster are recursively clustered. The algorithm terminates when the cluster size reaches a threshold. This data structure is similar to the kd-tree, but decompositions are performed across dimensions. During search, the tree is traversed by comparing the distance between the query vector and each cluster centroid. A priority queue of closest branches is maintained as the algorithm traverses each branch in the queue starting

from the closest center. Untraversed branches are added to the priority queue in the order of increasing distance to the query vector. This method does not guarantee exact searching as poor traversals could lead to falsely identifying neighbors in the wrong cluster. The level of approximation is controlled by the maximum number of branches to be visited. In our experiments, we used the default configuration of 32 centroids and 11 iterations per cluster step. We will refer to the priority search k-means approach simply as *k-means*.

2.3 Insights from FLANN

Approximate algorithms reduce the scope of a search, but not to $O(Q \times \log N)$: Approximate kNN algorithms prune the search space by using data structures. Unlike traditional database indices, these data structures trade-off accuracy for improved search time. Accuracy is defined as the set intersection of S_L and S_T where S_L is the set of values returned by linear search and S_T is the set of values returned by the approximate variants of kNN. Figure 2 shows the percentage of the dataset that must be searched in order to meet a fixed accuracy target for kd-trees and k-means. In this characterization, we use 100K image vectors and 32K query vectors. In order to achieve 90% accuracy, **at least 10%** of the dataset must be compared per query.

Constructing the index takes time: Prior to search, all feature vectors are placed in a kd-tree or a k-means data structure which is supposed to enable sublinear search time scaling with respect to data size. The cost of construction of this data structure is amortized by the number of searches performed over it. In

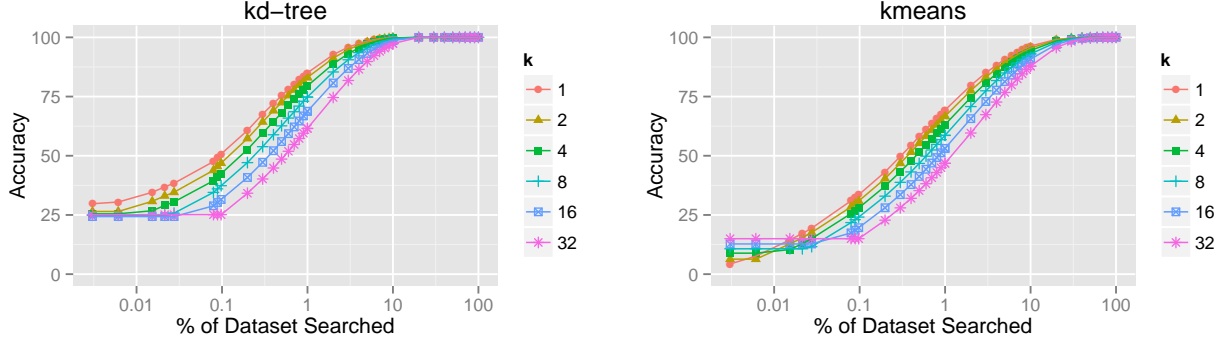


Figure 2: Accuracy as a function of % dataset searched: Approximate data structures reduce the scope of a search, but not logarithmic to the dataset size.

our study, building the data structure is about three orders of magnitude slower than performing a search. While search time grows linearly with the dimensionality of the data, the construction time grows linearly with both dimensionality and dataset size. The data structure should also adapt and be rebuilt when new content is added or deleted from the dataset, otherwise search accuracy will degrade. However, this process can be performed offline and removed from the critical path of application execution. We note that we do not evaluate accelerating the data structure creation process with the NCAM, although it can be used in that way.

Most of kNN search (with and without data structures) is distance computations: In linear search, effectively all of the execution time is devoted to pairwise distance calculations, while a tiny fraction is spent sorting the distances. For approximate kNN, the distance computation comprises 88.7% and 98.8% of execution time when using kd-trees and k-means, respectively. Distance calculations are performed at branch traversal. Branch-query distance calculations must be performed until a query hits the leaf nodes of the index. Once at the leaves, a final distance calculation from the query to the leaf node’s contents is performed.

The nearest neighbor algorithm is highly memory bound: For a brute-force linear scan, the computational intensity is 0.75 instructions/byte-moved and 2 instructions/byte-moved for Euclidean and Hamming distance, respectively. The interconnect bandwidth between DRAM and CPU is saturated well before the computation for a multi-core CPU.

2.4 Applications Design Points for kNN

How big is k ? Table 1 shows the values that the parameter k takes on for a variety of applications. The primary use-case depends on the task. In the kNN Classifier where $k = 1$, a query is labeled by the label of its single nearest neighbor; generally larger values of k are preferred to make the classifier more robust to noise. Lowe’s ratio test is a heuristic that prunes out noisy samples by rejecting outliers. It takes the ratio of the first and second closest neighbors, and if this ra-

tio is less than a threshold, the two returned features are not good matches. Other applications like content-based search [3], document retrieval [1], and motion planning [4] require the retrieval of many neighbors.

How many dimensions are used? Table 2 lists feature descriptors that are considered the state-of-the-art. The feature descriptor used defines the vector dimensionality or feature size of the database and queries. The use of a specific descriptor over another depends on the task. For example, a shape-based feature descriptor is optimal for distinguishing between different characters in the alphabet [31].

To simplify our discussion going forward, Table 3 lists three design points reflecting parameters typical of mobile and server kNN workloads. Our mobile design point is influenced by works that make extensive use of dimensionality reduction techniques [36] where accuracy is traded off for better energy and power efficiency. Our server design points are influenced by descriptors that have been shown to perform well for image retrieval tasks [37, 38].

3. THE NCAM ARCHITECTURE

In this section, we discuss the design and microarchitecture of the NCAM as shown in Figure 3. An NCAM memory module consists of a die stacked compute layer composed of *kNN accelerators* underneath a back end memory layer. In this paper we use an HMC interface die stacked memory as our back end memory substrate but our accelerator and design principles can be ported to other emerging memory interface specifications such

Application	k
Basic kNN Classifier	1
Lowe’s Ratio Test [32]	2
Document Distances [1]	1-19
Motion Planning [4]	15
Content-based Image Searching [this paper]	32

Table 1: Application values for k

Feature Descriptor	Dimensionality
SURF [33]	64
Word Embeddings [1]	50-100
SIFT [32]	128
GIST [34]	960
CNN-AlexNet [35]	4096

Table 2: Feature descriptors and their dimensionality

Design Point	Dimensionality	k
Mobile	64	2
Server-SIFT	128	16
Server-AlexNet	4096	32

Table 3: Design points used in our study

as High Bandwidth Memory (HBM) or emerging memory back ends such as Micron XPoint [39].

3.1 NCAM memory module

We use a Micron Hybrid Memory Cube (HMC) based memory as our memory substrate. The HMC is a memory specification for communicating with die-stacked DRAM based memory [40] typically with 4 or 8 layers. Under HMC, memory is organized vertically; a vertical cross section of memory is known as a *vault*. Each vault contains a set of DRAM memory banks with a *vault controller* located at the base logic layer. HMC provides up to $15\times$ the bandwidth of a DDR3 memory module while consuming 70% less power per bit [41].

For our design, we assume an HMC interface with 16 vaults each operating at 10 GB/s or 160 GB/s of aggregate internal bandwidth, and 60 GB/s of external bandwidth. Preliminary HMC prototype numbers show that a typical HMC interface memory operates at 11 W and has a 729 mm² die area [40]. Since the NCAM module integrates the kNN acceleration logic inside the memory module itself, it reaps the full benefits of the internal bandwidth speeds. Although the NCAM memory module must also support host communication, we will show later that the external bandwidth required by kNN is negligible.

Conceptually, the dataset vectors are preloaded offline into the HMC DRAM, and queries are loaded in the kNN acceleration logic. The computation starts when the dataset vectors from each vault’s memory banks are streamed into the NCAM logic layer where distance calculations are performed against the query vectors. Once all query-candidate scores are computed, the host processor aggregates the results into a global top-k buffer using an algorithm akin to selection sort (§5.1).

3.2 NCAM logic layer and microarchitecture

The NCAM *logic layer* is composed of both vault controllers that communicate with the memory vaults and kNN accelerators. Each vault controller is connected to one kNN accelerator which is responsible for processing

all data coming out of memory (Figure 3a). Each kNN accelerator is designed to service a maximum throughput that matches the 10 GB/s bandwidth from each vault controller. Since kNN accelerators are uniquely paired to vault controllers, data access is localized to each vault. This reduces latency variations resulting from non-uniform memory access, and eliminates global bank conflicts.

An individual kNN accelerator is composed of multiple kNN engines, each of which is responsible for processing a different query vector. For instance, if multiple query vectors are to be processed in parallel, a different query would be loaded into a different kNN engine. The exact number of parallel kNN engines per accelerator is a design parameter which can be adjusted according to the target application space of the NCAM module. A data arbitration unit is responsible for replicating the streams to drive each kNN engine in parallel.

kNN engine: Each kNN engine (Figure 3c) consists of several parallel *kNN processing units (PU)* which operate on multiple 32-bit wide data streams from memory, and a *query memory* that holds a buffer of queries to be broadcast to the PUs. In order to service the bandwidth supplied by the vault controllers, PUs are replicated in parallel to provide a sufficiently wide enough datapath to service the peak data rate (each PU services a different data stream). The exact number of PUs instantiated in parallel per kNN engine is a function of the operating frequency. For a PU throughput B_{pu} , each kNN engine would instantiate $(10\text{ GB/s})/B_{pu}$ PUs in parallel.

Query memory: The query memory holds the query vectors and generates a serialized query vector stream that is to be compared against the incoming data stream from the vault controllers; a small address controller is responsible for driving the query memory and indicating the end of each vector streamed into the processing unit. A write interface allows the host processor to load query vectors into memory prior to processing. For Euclidean distance, this module outputs one dimension of the query vector per cycle while for Hamming distance it outputs 32 dimensions per cycle (one bit per dimension).

kNN processing unit: A kNN processing unit (Figure 3d) takes as input a query stream and data stream, and consists of a *distance unit*, and a *priority queue*. Each PU processes a different 32-bit wide data stream from the memory. Since the computation is purely feed forward, the processing unit can process a new 32 bit value each cycle.

Distance unit: This module is responsible for computing the distance between query and candidate vectors. Vectors are streamed in 32 bits per cycle. Each query-candidate pair generates a tuple containing a distance score and the ID of the candidate vector. We evaluate Euclidean and Hamming distance units but any distance unit can also be implemented. The Euclidean distance unit consists of a subtract and multiply to generate a distance score which is sent to the accumulator. The Hamming distance unit processes 32 dimensions

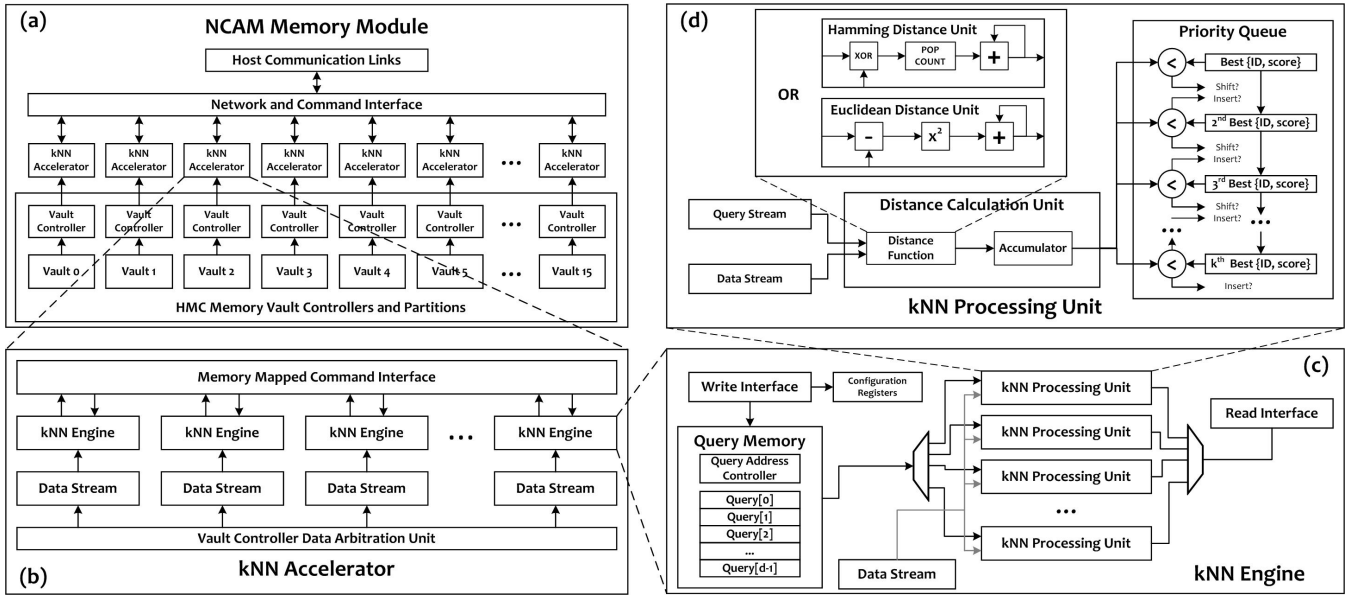


Figure 3: The NCAM architecture: An NCAM module (a) is composed of kNN accelerators (b) integrated per vault controller. Each kNN accelerator is composed of kNN engines (c) which are composed of kNN processing units (d). Each kNN processing unit is composed of a distance unit and a priority queue.

per cycle by performing a 32 bit XOR operation and population count to generate the distance score.

Priority queue: This module holds the top- k sets of candidate vector IDs and distance scores. The queue initializes each entry’s score to the maximum distance which allows the queue to initially start sorted. Each distance score and ID tuple generated by the distance unit is compared against the current set of top- k scores. If the new {score, ID} pair is better than entry i but worse than entry $i-1$, then all entries with higher scores at indices i to k are shifted to the next position in the queue. The new {score, ID} pair is then inserted at position i . Since we expect the number of desired neighbors k to remain relatively small and multiple comparisons need to be executed in parallel, we use registers to implement this module.

4. HARDWARE/SOFTWARE INTERFACE

4.1 Hardware interface

To program the NCAM, we use a memory mapped interface which maps configuration registers and memories in each kNN accelerator to a special address region dedicated to operating the NCAM. Each kNN accelerator is apportioned a small section of this memory region to expose its read and write interface to incoming host processor commands. These interfaces are used to set parameters such as vector dimensionality and the query vectors in the NCAM and to read the final results from the NCAM priority queues.

The NCAM hardware interface operates using a set of commands that are strictly an addition to existing memory interface command sets. This ensures that NCAM

operations can operate in parallel with existing commands and require no changes to the system memory controller. The NCAM command set consists of: IDLE, READ, WRITE, ENABLE, and DISABLE. A separate NCAM controller (not shown) is responsible for processing and configuring the NCAM accelerator based on the NCAM commands received.

4.2 Software interface

A kNN sample program is shown in Figure 4. The NCAM’s programming model abstracts away the low-level details of communicating to the NCAM. Similar to the CUDA programming model, we use analogous memory and execution operations to the NCAM memory: `nwrite_query`, `nmemcpy`, `nexec`, and `nread_result`. Pages with data subject to NCAM queries are pinned (not subject to swapping by the OS), and NCAM queries do not cross page boundaries. The NCAM enabled memory region is tracked and stored in a free list similar to how standard memory allocation is implemented in modern systems.

5. METHODOLOGY

We evaluate kNN performance on low- and high-power CPU and GPU platforms. For the CPU, we used the state-of-the-art FLANN [29] library. For the GPU, we use Garcia’s kNN implementation on the GPU [42] and extended Garcia’s benchmark to include Hamming distance calculations to evaluate both Euclidean and Hamming distance. Because approximate kNN algorithms require a large portion of the DB to be searched (§2.3), we evaluate using exact, linear kNN linear search and do not use any preprocessed data structures.


```

int * knn(int * query, int * dataset,
          size_t length, size_t dims, int k) {
    int * nbuf = nmalloc(length)
    nwrite_query(nbuf, query, dims)
    memcpy(nbuf, dataset, length * sizeof(int))
    nexec(nbuf)
    int * result = nread_result(nbuf)
    nfree(nbuf)
    return result
}

```

Figure 4: Example program using NCAM enabled memory: Because the NCAM is specialized to perform kNN, many lower-level hardware primitives can be hidden from the programmer.

5.1 NCAM methodology

To evaluate the NCAM, we build an analytical model using ASIC post-placement and route estimates. The model estimates execution time as a function of NCAM execution time, host processing time, and global top-k reduction time. We implement six NCAM designs, one for each design point listed in Table 3 for Hamming and Euclidean distance. We include upper-bounds for host-processing overheads when communicating to and from the NCAM. We assume that the candidate vectors are already resident inside the HMC DRAM. NCAM execution time starts when a query is issued, and ends when the global top-k results are written to system DRAM. We detail our analytical model below.

Power and Area: We estimate the performance, area, and power consumption of the NCAM using post-placement and route estimates generated by the Synopsys Design Compiler, IC Compiler, and PrimeTime using a TSMC 65 nm library. Because the CPUs and GPUs are implemented in a newer 28 or 32 nm technology, we compensate by adjusting the NCAM power and area results by a factor of two. Prior work shows an appropriate scaling is $2\text{--}3\times$ [43–45], and hence we stick to the conservative end of this range. For each design point, we implement a Hamming distance and a Euclidean distance accelerator across a range of frequencies (125MHz, 250MHz, 500MHz, 800MHz) for each of the design points in Table 3. Because the kNN PUs process 32-bit words per cycle, the throughput of each kNN PU BW_{lane} is proportional to the operating frequency f times the data width.

To estimate the total power and area overheads of the NCAM, we first estimate the area overhead of a single NCAM accelerator; for simplicity we fix the number of kNN engines per kNN accelerator to one. We estimate the total power of the NCAM P_{ncam} by taking the power for on kNN engine $P_{accelerator}$ and multiplying it by 16 (the number of vaults on the HMC memory). Similarly to estimate the total area incurred by the NCAM acceleration logic, we take the area for on kNN accelerator $A_{accelerator}$ and multiply by 16. The runtime associated with streaming the data through the NCAM $t_{euclidean}$ for the Euclidean distance, and $t_{hamming}$ for

the Hamming distance is then just the dataset size divided by the internal HMC bandwidth.

Host-processing overhead: The NCAM is analogous to an accelerator where it is controlled by a host CPU. Thus, we account for host processing overheads by modeling a host program that performs reads and writes on the NCAM from DRAM. For the ARM Cortex A15, we add cache miss latency penalties [46] to account for uncached accesses when communicating with the NCAM. For the Xeon E5-2620, we flush each memory reference for the NCAM using the `clflush` instruction. These estimates are an upper bound for the time required to move the query vectors to the memory mapped locations on the NCAM, and read results from memory from the priority queues. For each kNN engine, only a single D dimensional vector needs to be moved to the NCAM since a single query memory drives each of its local R PUs. Our host processing program consists of writing the query vector to memory, reading the results, and aggregating the global top k -nearest neighbors. The estimated $t_{hamming}$ or $t_{euclidean}$ is then added to the runtime of the host processing program t_{host} . When writing the query vectors, our host processing program applies a memory fence before proceeding to read and aggregate the results from memory.

We compute the total single query latency t_{total} by computing $t_{ncam} + t_{host}$. The throughput per watt T_{total} for the NCAM is calculated by taking the number of queries serviced divided by the energy required to service the queries. If the energy required to service q queries is $t_{ncam} \times P_{ncam} + t_{host} \times P_{host}$, then the throughput per watt $T_{ncam} = q / (P_{ncam} + t_{host} \times P_{host})$.

Sorting local top-k queues into global top-k: To read the results from the NCAM, the host process must sort the results from each kNN PU (each PU has a set of k sorted local results). For an NCAM with R total PUs across all 16 kNN engines, only $R + k - 1$ results need to be read from the NCAM since we only need to retrieve the top- k global nearest neighbors. To do this, the host processor creates a set S of only the first {score, ID} pair from each kNN PU, and the best {score, id} pair in S is selected as the global nearest neighbor (say from the Q th kNN PU). The closest neighbor is removed from S and the 2nd closest neighbor in the Q th PU is read from the NCAM and added to the set S . The selection then chooses the 2nd global closest neighbor by again choosing the best {score, ID} pair in S and repeats the process until the global top- k neighbors have been selected. Notice that in this result retrieval stage, the number of reads scales linearly with k or R , instead of scaling linearly with both R and k if we read all the local results then sorted them.

5.2 Multi-core CPU methodology

We evaluate the mobile design point using a quad core ARM Cortex A15 CPU on a Jetson TK1 SoC. For Server-SIFT and Server-AlexNet, we use an Intel Xeon E5-2620 processor with AVX extensions enabled. To evaluate throughput per watt, we use the FLANN library which provides both Hamming and Euclidean

space vector representations. We configure FLANN to process a batch $q = 4096$ queries in parallel against datasets which are sufficiently large enough to eliminate cache effects, and measure the total runtime t_{cpu} for each CPU platform using FLANN’s linear brute force search. We use different dataset sizes and scale appropriately for different platforms since memory capacity and cache sizes vary. Using a power meter, we measure the compute power P_{cpu} by measuring the average power of the entire server during peak load, and subtracting the idle power. The throughput per watt T_{cpu} is then calculated as $T_{cpu} = q/(P_{cpu} \times t_{cpu})$. FLANN only supports query-level parallelism and is therefore not optimized for latency. In order to make a fair comparison, we wrote our own custom latency optimized kNN implementation which parallelizes across dataset vectors instead; the latency L_{cpu} is then recorded by measuring the runtime of our latency-optimized kNN implementation.

5.3 GPU methodology

We evaluate both throughput per watt and latency for GPUs. We used a NVIDIA Jetson TK1 and an NVIDIA Titan X. For the mobile design points, we use the Jetson TK1 GPU which has 192 CUDA cores. To evaluate Server-SIFT and Server-AlexNet, we use a Titan X with 3072 CUDA cores. We evaluate the GPU using Garcia’s GPU kNN library [42]. To compute the throughput per watt for the GPU, we record the runtime t_{gpu} by measuring the execution time of the GPU using a 1 million item dataset for a batch size of $q = 4096$ queries; we measure the GPU compute power P_{gpu} by recording the difference between idle and load power using the on-board NVIDIA power meters. The effective throughput per Watt T_{gpu} is then calculated as $T_{gpu} = q/(P_{gpu} \times t_{gpu})$. To measure the latency of the GPU L_{gpu} , we measure the runtime of the GPU to process a single query.

6. EVALUATION

We evaluate the throughput per watt and latency of the NCAM relative to CPU and GPU systems and show it is more energy efficient than existing solutions. We first present and evaluate the power and area overhead estimates of the NCAM and show that our design overheads are compatible with memory substrates like HMC. Finally, we compare the performance of the NCAM against a recent commercial PIM platform, the Micron Automata Processor, for Hamming Distance kNN search.

6.1 Performance, power, and area

Table 4 shows our power measurements for the CPU and GPU. Table 5 shows energy efficiency, power, and area estimates for each of the six NCAM design points at 800 MHz. Figures 6 and 5 show NCAM latency and throughput. We describe our evaluation below.

Throughput: To evaluate throughput per watt, we use the power measurements shown in Table 4. We report throughput per watt for each platform relative to

Parameter	Idle Power (W)	Load Power (W)
NVIDIA Jetson TK1 (P_{gpu})	5	8.5
NVIDIA Titan X (P_{gpu})	20	153
ARM Cortex A15 (P_{cpu})	5	13.5
ARM Cortex A15 (P_{host})	4.8	7.3
Intel Xeon E5-2620 (P_{cpu})	182	244
Intel Xeon E5-2620 (P_{host})	180	196

Table 4: Power measurements for CPU and GPU platforms.

the NCAM in Figure 5. For each NCAM design, we use the frequency which produces the highest throughput per watt when evaluating against the CPU and GPU. Our results show that the NCAM can achieve up to three orders of magnitude improvement over multi-core CPU systems for both Hamming and Euclidean space kNN. The NCAM can also achieve 8.5-160 \times throughput per watt improvement over the Titan X GPU and up to 21 \times energy efficiency over the Jetson TK1 GPU.

Latency: We evaluate the latency of a single query across each platform to determine the potential impact of the NCAM in latency-sensitive environments. Our results show the NCAM can achieve up to 17 \times and 128 \times latency improvement over the CPU and GPU, respectively (in the Euclidean space kNN). We attribute this speedup from both increased memory bandwidth and the use of specialized hardware. Increased memory bandwidth alone accounts for a 6 \times improvement.

The remaining improvements (two to three orders of magnitude) come from specialization. Energy efficiency remains unchanged since reducing the bandwidth also reduces the computation required. For Hamming space kNN, our results show that we can achieve up to two orders of magnitude over the CPU and three orders of magnitude over the GPU. This is because the GPU does not have enough work to perform latency-hiding across warps. On the other hand, the NCAM is a latency-optimized design which is able to operate at full throughput even for small data sizes.

Power and Area: We performed frequency sweeps for $f = 125, 250, 500, 800$ MHz. Across frequencies, the total estimated NCAM power consumption remain relatively flat (not shown). This is because each design point targets fixed throughput so a design operating at 500 MHz will incur roughly twice the area at half the power of a design operating at 250MHz.

In terms of area footprint, our designs incurs less than 1% area overhead compared to the area of the HMC logic layer. Our results also show the acceleration logic requires at most 1.7 W of power which is about 15% of the die-stacked memory power for HMC (11 W). The largest of our designs (Hamming Server-AlexNet) incurs 1.37 mm^2 or less than 0.19% of the HMC total die area (729 mm^2), while the smallest of our design points (Mobile) requires 0.20 mm^2 or less than 0.03% overhead. Our area estimates also show that the Hamming accelerators are commensurate in size to their Eu-

Design Point	Throughput per watt (Queries per Joule)	Latency per query (ms)	Power (W)	Distance Unit (mm ²)	Priority Queue (mm ²)	Query Memory (mm ²)	Total Area (mm ²)
Euclidean Mobile	55104	.0157	0.53	0.23	0.079	0.022	0.34
Hamming Mobile	57811	.0139	0.39	0.10	0.10	0.002	0.20
Euclidean Server-SIFT	429	3.39	0.96	0.23	0.50	0.022	0.73
Hamming Server-SIFT	5186	0.12	0.72	0.16	0.38	0.003	0.55
Euclidean Server-AlexNet	10.2	108	1.25	0.25	0.83	0.062	1.14
Hamming Server-AlexNet	0.68	3.39	1.68	0.31	1.04	0.018	1.37

Table 5: Energy efficiency, latency, and area for various NCAM designs at 800 MHz

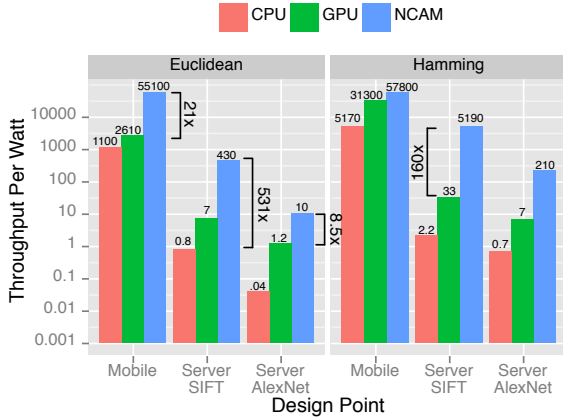


Figure 5: Throughput per watt (Queries/Joule)

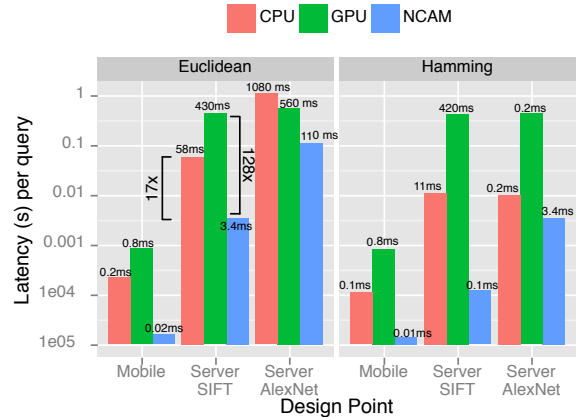


Figure 6: Latency for a single query

clidean counterparts. This is because the difference in size between the Hamming distance unit and Euclidean distance unit is dominated by the size of the priority queues. The priority queue composes a non-trivial fraction of the design area for both the Hamming and Euclidean distance implementations.

Host processing overhead: We report the estimated NCAM runtime with host processing overheads using the methodology outlined in Section 5. Our results (not shown) indicate that for the mobile design points, the NCAM is limited by the host processing latency which accounts for upwards of 99% of the processing time. This is because the size of the mobile dataset in these applications fits in cache which inflates CPU and GPU performance while the NCAM pessimistically pays a full DRAM cache miss for every memory reference. For larger datasets and workloads, we show that the host processing time is negligible and execution time is dominated by the NCAM latency. With future memory technologies, we expect the latency from the host processor to memory to be substantially reduced which will alleviate this bottleneck for the mobile NCAM design point.

6.2 Micron Automata Processor

We also evaluate the NCAM against the Micron Automata Processor (AP) which is one of the most recent commercialized PIM architectures [47]. The AP is a non-von Neumann architecture that uses a non-deterministic finite automata (NFA) driven execution model. Programmers specify one or multiple NFAs which are mapped and executed on AP processors in a similar fashion to FPGAs. Our evaluation finds that it is possible to implement arithmetic operations on the AP, but is inefficient in practice. Thus, we rule out Euclidean distance based kNN which requires adders and multipliers, and instead focus on Hamming distance kNN which requires only bitwise XOR and population count operations.

Our AP kNN design encodes the dataset vectors in the AP’s state transition elements (STEs) where one unique Hamming distance NFA is generated per data vector [48]. Query vectors are streamed in to each Hamming distance in parallel effectively evaluating the score over all dataset vectors in parallel. We then use a race logic sort [49] to perform the reduction among different Hamming NFAs and determine the k best scores. The key insight is that instead of computing the Hamming distance $H(x)$ for a d -dimensional vector x , we compute $d - H(x)$ which is computed using counters on the

Workload	Blocks Per Macro	Features Per 32 Chips	Freq (MHz)	Reconfigs.	t_{stream} (s)	t_{config} (s)	MAP Query / J with config	MAP Query / J w/o config	NCAM Query / J
Small	2	1024	133	0	0	0.001	7932	7932	57810
Medium	5	1228	133	853	38.39	1.71	0.20	4.67	5187
Large	2118	3	65.5	361471	16266	45631	0.00013	0.000175	211

Table 6: Hamming distance AP comparison

AP. We then uniformly increment each counter in each Hamming NFA to race to the value $d + 1$. The first k counters to surpass the threshold are the top k nearest neighbors. When the dataset does not fit in AP memory, we rely on dynamic reconfiguration of the board to load different sets of Hamming NFAs.

We implement, compile, place, and route our Hamming distance NFAs using the Automata Network Markup Language (ANML) and AP SDK to build an analytical model of the AP’s performance. We assume an AP configuration of 32 AP chips operating at 128 W [50]; each AP chip has two half-cores which contain 96 blocks each (6144 blocks total). Our design requires $q * (2d + (1/2) \log_2(d))$ cycles to stream in and process a d dimensional vector for q queries. To compute how many board reconfigurations are needed, we calculate the blocks B_{macro} required for a single Hamming NFA and compute the number of board reconfigurations for N vectors $C = \lceil N \times B_{\text{macro}} / 6144 \rceil$. One reconfiguration takes 0.045 s [51] so the total reconfiguration overhead takes $t_{\text{config}} = 0.045(C - 1)$. The energy efficiency is then just $T_{\text{ap}} = (t_{\text{config}} + t_{\text{stream}}) \times 128$ J/s shown in Table 6. Since the reconfiguration overhead is amortized by the number of queries, we report two numbers: the energy efficiency with reconfiguration overhead and energy efficiency without reconfiguration overhead (an upper bound on energy efficiency).

Our analytical model shows the current generation AP would perform orders of magnitude worse than the NCAM. We attribute the shortcomings of the AP compared to the NCAM to the following reasons. First, the AP is unable to capitalize on large datapaths for the Hamming distance calculations; unlike our NCAM design which can perform an XOR and population count on a 32 bit wide datapath, the AP is limited to processing 1 bit per cycle since AP counters only increment by one. Second, we find that the AP is inefficient for large dataset cardinality or feature vector dimensionality. This is because for large datasets the reconfiguration time dominates execution time, and for high dimensionality the Hamming NFAs require significant resources even though only a few states will be active at any given time. Third, we find that unlike the NCAM which supports arbitrary dimensional vectors, the vector dimensionality the AP can support is limited by the maximum automata size. This is because the size of the Hamming NFAs scale with dimensionality and cardinality on the AP unlike the NCAM which uses a streaming distance calculation (constant resources per distance unit). Finally, our model uses an early revision of the

AP platform and estimated TDP power which is typically higher than measured dynamic power; we expect that future generation APs will enjoy clock frequency, power, and reconfiguration latency improvements both from optimization efforts and technology scaling [52].

7. DISCUSSION

Specialization for kNN search: As Moore’s law nears its end, power limitations of CMOS technology have accelerated the push towards specialization and domain-specific architectures [53]. It is not unprecedented to build specialized accelerators for vitally important applications or when general purpose processing fails to meet viable performance targets. For example, CAMs or TCAMs are widely used to accelerate high speed pattern matching to meet extremely tight latency constraints. On the other hand, custom ASICs like the CM1K neuromorphic accelerator [54] aim to reduce the expensive neural network computations used for recognition tasks to an embedded form factor. Because kNN is a common primitive to many contemporary applications (e.g., machine learning), specialization is well warranted and not unreasonable as results show general purpose architectures are ill-suited to such a task.

Interestingly, our specialized NCAM is capable of functioning as a regular content addressable memory (CAM). This is done by setting $k = 1$ and then performing a quick equality check at the end. It can also operate as a ternary CAM (TCAM) by adding a two-bit Hamming distance calculation unit (for ternary matching). So in addition to specialization benefits of NCAM, one can use it as a more general functional unit.

Hamming vs. Euclidean distance metrics: The NCAM can improve the throughput per watt for Euclidean space kNN search by $531\times$ over the CPU. For Hamming space kNN, the NCAM can improve energy efficiency by three orders of magnitude. This performance improvement is attributed to the highly efficient and parallelized XOR and population count implementation in the NCAM accelerator.

Fixed point representations can achieve a portion of these gains from hardware specialization and algorithm co-design. Our results using a Euclidean distance accelerator and Hamming distance accelerator correspond to the upper and lower bound respectively on energy and performance improvements that can be made across the NCAM design space. Using fixed point representations between 1 and 32 bits of precision will achieve similar improvements in both energy efficiency and latency.

Scaling beyond $k > 32$: Our evaluation targets relatively low k values for the kNN algorithm. It is possible to support higher k values with low overhead. The first solution is to increase the size of the priority queue to expand the capacity of each NCAM. A second solution is to replace the priority queue in the PU with a module that performs a k -selection algorithm; this requires the host processor to sort more data when aggregating. A third solution is to search using NCAMs in rounds with a fixed priority queue size k' ; in this solution, the top k nearest neighbors are computed in k/k' rounds where each round computes k' results and deletes them from the dataset before the next round of search.

We argue that using k -selection or increasing the priority queue size are unnecessary solutions; searching in rounds and temporarily deleting elements does not scale to multiple queries operating in parallel. Instead, using a relatively small priority queue depth $k' < k$ is sufficient for most applications where the size of the dataset is much larger than k . The key insight is that the probability that more than k' of the global top k elements are on the same NCAM module is negligible and only becomes significant when the size of the dataset becomes on the order of k at which point the sorting overhead becomes significant. In the common case, one round of search will be sufficient since the set of all locally computed k' nearest neighbors across NCAMs is highly likely to contain the global top k nearest neighbors. In the extreme case where the first round of search fails, a second round of search would be executed.

8. RELATED WORK

The concept of near-data processing has been studied in the literature for decades [55]. More interestingly, the concept of tightly integrating nearest neighbor search accelerators into memory also has an established history, indicating ongoing interest.

CAMs: As far back as the 1980s and 1990s, near-memory accelerators were proposed to improve the performance of nearest neighbor search using CAMs [56] and tightly coupled DRAM accelerators [57]. Kohonen et al. [58] proposed using a combination of CAMs and hashing techniques to perform nearest neighbor search. Kanerva et al. [59] propose sparse distributed memory (SDM) and a “Best Match Machine” to implement nearest neighbor search; the ideas behind SDM were later employed by Roberts in his design [56] which is, to the best of our knowledge, the first proposed CAM based accelerator capable of performing nearest neighbor search on its own. His design, called proximity CAM (PCAM), was fabricated using $2\mu\text{m}$ CMOS technology and demonstrated several orders of magnitude performance improvement.

Algorithms that exploit TCAMs perform content addressable search such as ternary locality sensitive hashing (TLSH) [60] and binary-reflected Gray code [61] do exist. However, TCAMs suffer from lower memory density, higher power consumption, and smaller capacity than emerging memory technologies. While prior work [62] shows promising increases in performance, en-

ergy efficiency, and capacity, TCAM cells are less dense than DRAM cells. For the massive scale datasets in kNN workloads, the density disparity translates to an order of magnitude in cost. Despite these limitations, there is still active work in TCAMs for data-intensive applications; Guo et al. [63] propose AC-DIMM which augments TCAM memories to accelerate associative computing applications like key-value store.

PIMs & Accelerators: Patterson et al. [64] propose IRAM which introduces processing units integrated with DRAM to exploit higher internal bandwidth and achieve reduced memory latencies. Kogge et al. [65] propose the EXECUBE architecture which integrates general purpose cores with DRAM macros. Deering et al. [66] propose FBRAM, a “new form” of memory optimized to improve random access writes to accelerate z-buffering for 3D graphics algorithms. Elliott et al. [67] propose C-RAM which add SIMD processing units adjacent to the sense amplifiers capable of bit serial operations. Active Pages [14] and FlexRAM [11] envision a programmable processing element near each DRAM macro block which could be programmed for kNN acceleration. However, none of these prior efforts directly addresses the kNN search problems we discuss.

Lipman and Yang [57] propose a DRAM based architecture called smart access memory (SAM) for nearest-neighbor search targeting DB applications. Their design tightly integrates a k -nearest neighbor accelerator engine and microarchitecturally shares common elements with our design; however, they do not contextualize their accelerator within the space of kNN applications and do not evaluate the design space trade offs in power and area. Agrawal et al. [68] exploit accelerators to reduce the total cost of ownership of high-dimensional similarity search. Yu et al. [69] optimize all-pairs nearest neighbors by fusing neighbor selection with distance computations. Finally, Tandon et al [2] propose an all pairs similarity accelerator for NLP; however, unlike our work they integrate their accelerator with the last level cache not memory.

9. CONCLUSIONS

While we use DRAM as our memory substrate for the NCAM presented in this paper, the high level design paradigms and insights still generalize to alternative memory technologies and in-memory processing architectures. For example, emerging technologies such as the Micron Hybrid Memory Cube (HMC) [16] or new interface specifications such as High Bandwidth Memory (HBM) [70] present new exciting memory substrates where the NCAM accelerator can be ported. The PIM techniques presented in this paper are also relevant to other data intensive machine learning and computer vision applications today where data movement is an increasingly fundamental challenge in improving energy efficiency. Our work shows one example of how PIM can accelerate these machine learning applications in the context of kNN, however there exist many more opportunities where PIM can provide orders of magnitude performance and energy improvement.

10. REFERENCES

- [1] M. Kusner, Y. Sun, N. Kolkin, and K. Q. Weinberger, "From Word Embeddings To Document Distances", in *Proceedings of the 32nd International Conference on Machine Learning (ICML-15)* (D. Blei and F. Bach, eds.), pp. 957–966, JMLR Workshop and Conference Proceedings, 2015.
- [2] P. Tandon, J. Chang, R. G. Dreslinski, V. Qazvinian, P. Ranganathan, and T. F. Wenisch, "Hardware acceleration for similarity measurement in natural language processing," in *Proceedings of the 2013 International Symposium on Low Power Electronics and Design, ISLPED '13*, (Piscataway, NJ, USA), pp. 409–414, IEEE Press, 2013.
- [3] Y. Liu, D. Zhang, G. Lu, and W.-Y. Ma, "A survey of content-based image retrieval with high-level semantics," *Pattern Recognition*, vol. 40, no. 1, pp. 262 – 282, 2007.
- [4] A. Yershova and S. LaValle, "Improving Motion-Planning Algorithms by Efficient Nearest-Neighbor Searching," *Robotics, IEEE Transactions on*, vol. 23, pp. 151–157, Feb 2007.
- [5] P. Indyk and R. Motwani, "Approximate nearest neighbors: Towards removing the curse of dimensionality," in *Proceedings of the Thirtieth Annual ACM Symposium on Theory of Computing, STOC '98*, (New York, NY, USA), pp. 604–613, ACM, 1998.
- [6] M. Datar, N. Immorlica, P. Indyk, and V. S. Mirrokni, "Locality-sensitive hashing scheme based on p-stable distributions," in *Proceedings of the Twentieth Annual Symposium on Computational Geometry, SCG '04*, (New York, NY, USA), pp. 253–262, ACM, 2004.
- [7] A. Gionis, P. Indyk, R. Motwani, *et al.*, "Similarity search in high dimensions via hashing," in *VLDB*, vol. 99, pp. 518–529, 1999.
- [8] R. Weber, H.-J. Schek, and S. Blott, "A quantitative analysis and performance study for similarity-search methods in high-dimensional spaces," in *VLDB*, vol. 98, pp. 194–205, 1998.
- [9] W. A. Wulf and S. A. McKee, "Hitting the memory wall: Implications of the obvious," *SIGARCH Comput. Archit. News*, vol. 23, pp. 20–24, Mar. 1995.
- [10] D. Patterson, T. Anderson, N. Cardwell, R. Fromm, K. Keeton, C. Kozyrakis, R. Thomas, and K. Yelick, "A case for intelligent ram," *IEEE Micro*, vol. 17, pp. 34–44, Mar. 1997.
- [11] Y. Kang, W. Huang, S.-M. Yoo, D. Keen, Z. Ge, V. Lam, P. Pattnaik, and J. Torrellas, "Flexram: toward an advanced intelligent memory system," in *Computer Design, 1999. (ICCD '99) International Conference on*, pp. 192–201, 1999.
- [12] J. Draper, J. Chame, M. Hall, C. Steele, T. Barrett, J. LaCoss, J. Granacki, J. Shin, C. Chen, C. W. Kang, I. Kim, and G. Daglikoca, "The architecture of the diva processing-in-memory chip," in *Proceedings of the 16th International Conference on Supercomputing, ICS '02*, (New York, NY, USA), pp. 14–25, ACM, 2002.
- [13] J. Carter, W. Hsieh, L. Stoller, M. Swanson, L. Zhang, E. Brunvand, A. Davis, C.-C. Kuo, R. Kuramkote, M. Parker, L. Schaelicke, and T. Tateyama, "Impulse: building a smarter memory controller," in *High-Performance Computer Architecture, 1999. Proceedings. Fifth International Symposium On*, pp. 70–79, Jan 1999.
- [14] M. Oskin, F. T. Chong, and T. Sherwood, "Active pages: A computation model for intelligent memory," *SIGARCH Comput. Archit. News*, vol. 26, pp. 192–203, Apr. 1998.
- [15] IBM, "Blue Logic SA-27E ASIC," 1999. "http://www.ic72.com/pdf/s/381279.pdf".
- [16] J. T. Pawlowski, "Hybrid memory cube (hmc)," *Hot Chips*, vol. 23, 2011.
- [17] Jia, Yangqing and Shelhamer, Evan and Donahue, Jeff and Karayev, Sergey and Long, Jonathan and Girshick, Ross and Guadarrama, Sergio and Darrell, Trevor, "Caffe: Convolutional Architecture for Fast Feature Embedding," *arXiv preprint arXiv:1408.5093*, 2014.
- [18] J. Hauswald, M. A. Laurenzano, Y. Zhang, C. Li, A. Rovinski, A. Khurana, R. Dreslinski, T. Mudge, V. Petrucci, L. Tang, and J. Mars, "Sirius: An open end-to-end voice and vision personal assistant and its implications for future warehouse scale computers," in *Proceedings of the Twentieth International Conference on Architectural Support for Programming Languages and Operating Systems (ASPLOS)*, ASPLOS '15, (New York, NY, USA), ACM, 2015. Acceptance Rate: 17
- [19] Z. Du, R. Fasthuber, T. Chen, P. Ienne, L. Li, T. Luo, X. Feng, Y. Chen, and O. Temam, "Shidiannao: Shifting vision processing closer to the sensor," in *Proceedings of the 42nd Annual International Symposium on Computer Architecture, ISCA '15*, (New York, NY, USA), pp. 92–104, ACM, 2015.
- [20] J. Hauswald, Y. Kang, M. A. Laurenzano, Q. Chen, C. Li, R. Dreslinski, T. Mudge, J. Mars, and L. Tang, "Djinn and tonic: Dnn as a service and its implications for future warehouse scale computers," in *Proceedings of the 42nd Annual International Symposium on Computer Architecture (ISCA)*, ISCA '15, (New York, NY, USA), ACM, 2015. Acceptance Rate: 19
- [21] T. Chen, Z. Du, N. Sun, J. Wang, C. Wu, Y. Chen, and O. Temam, "Diannao: A small-footprint high-throughput accelerator for ubiquitous machine-learning," *SIGARCH Comput. Archit. News*, vol. 42, pp. 269–284, Feb. 2014.
- [22] Y. Chen, T. Luo, S. Liu, S. Zhang, L. He, J. Wang, L. Li, T. Chen, Z. Xu, N. Sun, and O. Temam, "Dadiannao: A machine-learning supercomputer," in *Microarchitecture (MICRO), 2014 47th Annual IEEE/ACM International Symposium on*, pp. 609–622, Dec 2014.
- [23] A. Gionis, P. Indyk, and R. Motwani, "Similarity Search in High Dimensions via Hashing," in *Proceedings of the 25th International Conference on Very Large Data Bases, VLDB '99*, (San Francisco, CA, USA), pp. 518–529, Morgan Kaufmann Publishers Inc., 1999.
- [24] M. Raginsky and S. Lazebnik, "Locality-sensitive binary codes from shift-invariant kernels," in *Advances in Neural Information Processing Systems 22* (Y. Bengio, D. Schuurmans, J. Lafferty, C. Williams, and A. Culotta, eds.), pp. 1509–1517, Curran Associates, Inc., 2009.
- [25] M. M. B. C. Strecha, A. M. Bronstein and P. Fua, "LDAHash: Improved Matching with Smaller Descriptors," *IEEE Transactions on Pattern Analysis and Machine Intelligence*, vol. 34, no. 1, 2012.
- [26] A. Torralba, R. Fergus, and Y. Weiss, "Small codes and large image databases for recognition," in *In Proceedings of the IEEE Conf on Computer Vision and Pattern Recognition*, 2008.
- [27] J. Wang, S. Kumar, and S.-F. Chang, "Semi-Supervised Hashing for Large-Scale Search," *IEEE Trans. Pattern Anal. Mach. Intell.*, vol. 34, pp. 2393–2406, Dec. 2012.
- [28] Y. Weiss, A. Torralba, and R. Fergus, "Spectral Hashing," in *Advances in Neural Information Processing Systems 21* (D. Koller, D. Schuurmans, Y. Bengio, and L. Bottou, eds.), pp. 1753–1760, Curran Associates, Inc., 2009.
- [29] M. Muja and D. G. Lowe, "Scalable Nearest Neighbor Algorithms for High Dimensional Data," *Pattern Analysis and Machine Intelligence, IEEE Transactions on*, vol. 36, 2014.
- [30] Yahoo!, "Webscope | Yahoo Labs," 2014.
- [31] S. Belongie, J. Malik, and J. Puzicha, "Matching shapes," in *Computer Vision, 2001. ICCV 2001. Proceedings. Eighth IEEE International Conference on*, vol. 1, pp. 454–461 vol.1, 2001.
- [32] D. G. Lowe, "Distinctive Image Features from Scale-Invariant Keypoints," *Int. J. Comput. Vision*, vol. 60, pp. 91–110, Nov. 2004.
- [33] H. Bay, A. Ess, T. Tuytelaars, and L. V. Gool, "Speeded-up robust features (surf)," *Computer Vision and Image Understanding*, vol. 110, no. 3, pp. 346 – 359, 2008.

Similarity Matching in Computer Vision and Multimedia.

- [34] M. Douze, H. Jégou, H. Sandhawalia, L. Amsaleg, and C. Schmid, "Evaluation of GIST Descriptors for Web-scale Image Search," in *Proceedings of the ACM International Conference on Image and Video Retrieval*, CIVR '09, (New York, NY, USA), pp. 19:1–19:8, ACM, 2009.
- [35] A. Krizhevsky, I. Sutskever, and G. E. Hinton, "ImageNet Classification with Deep Convolutional Neural Networks," in *Advances in Neural Information Processing Systems 25* (F. Pereira, C. Burges, L. Bottou, and K. Weinberger, eds.), pp. 1097–1105, Curran Associates, Inc., 2012.
- [36] G. Takacs, V. Chandrasekhar, N. Gelfand, Y. Xiong, W.-C. Chen, T. Bismipigiannis, R. Grzeszczuk, K. Pulli, and B. Girod, "Outdoors Augmented Reality on Mobile Phone Using Loxel-based Visual Feature Organization," in *Proceedings of the 1st ACM International Conference on Multimedia Information Retrieval*, MIR '08, (New York, NY, USA), pp. 427–434, ACM, 2008.
- [37] S. Agarwal, Y. Furukawa, N. Snavely, I. Simon, B. Curless, S. M. Seitz, and R. Szeliski, "Building Rome in a Day," *Commun. ACM*, vol. 54, pp. 105–112, Oct. 2011.
- [38] A. Babenko, A. Slesarev, A. Chigorin, and V. S. Lempitsky, "Neural Codes for Image Retrieval," *CoRR*, vol. abs/1404.1777, 2014.
- [39] Micron, "3D XPoint Technology," 2015. <http://www.micron.com/about/innovations/3d-xpoint-technology>.
- [40] H. M. C. Consortium, "Hybrid Memory Cube Specification 1.0," 2013.
- [41] H. M. C. Consortium, "Hybrid Memory Cube Consortium - The Technology," 2015.
- [42] V. Garcia, E. Debreuve, and M. Barlaud, "Fast k nearest neighbor search using GPU," in *Computer Vision and Pattern Recognition Workshops, 2008. CVPRW '08. IEEE Computer Society Conference on*, pp. 1–6, June 2008.
- [43] W. Zhao, *Predictive Technology Modeling for Scaled CMOS*. ProQuest, 2009.
- [44] S.-Y. Wu, J. Liaw, C. Lin, M. Chiang, C. Yang, J. Cheng, M. Tsai, M. Liu, P. Wu, C. Chang, L. Hu, C. Lin, H. Chen, S. Chang, S. Wang, P. Tong, Y. Hsieh, K. Pan, C. Hsieh, C. Chen, C. Yao, C. Chen, T. Lee, C. Chang, H. Lin, S. Chen, J. Shieh, M. Tsai, S. Jang, K. Chen, Y. Ku, Y. See, and W. Lo, "A highly manufacturable 28nm CMOS low power platform technology with fully functional 64Mb SRAM using dual/tripe gate oxide process," in *VLSI Technology, 2009 Symposium on*, pp. 210–211, June 2009.
- [45] B. Durga Prasad and N. Krishna, "Synthesis of a TI MSP430 microcontroller core using Multi-Voltage methodology," in *Communication Control and Computing Technologies (ICCCCT), 2010 IEEE International Conference on*, pp. 93–97, Oct 2010.
- [46] 7-CPU, "ARM Cortex-A15," <http://www.7-cpu.com/cpu/Cortex-A15.html>.
- [47] P. Dlugosch, D. Brown, P. Glendenning, M. Leventhal, and H. Noyes, "An efficient and scalable semiconductor architecture for parallel automata processing," *Parallel and Distributed Systems, IEEE Transactions on*, vol. 25, no. 12, pp. 3088–3098, 2014.
- [48] Micron, "Calculating Hamming Distance," http://www.micronautomata.com/documentation/cookbook/c_hamming_distance.html. Accessed: 2016-03-18.
- [49] A. Madhavan, T. Sherwood, and D. Strukov, "Race logic: A hardware acceleration for dynamic programming algorithms," in *Proceeding of the 41st Annual International Symposium on Computer Architecture*, ISCA '14, (Piscataway, NJ, USA), pp. 517–528, IEEE Press, 2014.
- [50] B. H. Noyes, "Micron's Automata Processor Architecture: Reconfigurable and Massively Parallel Automata Processing," 2014.
- [51] K. Wang, Y. Qi, J. J. Fox, M. R. Stan, and K. Skadron, "Association rule mining with the micron automata processor," in *Parallel and Distributed Processing Symposium (IPDPS), 2015 IEEE International*, pp. 689–699, IEEE, 2015.
- [52] "Discussion with micron automata processor team (dan skinner, matt tanner, matt grimm, terry leslie)." Private Communication. March 23rd, 2016.
- [53] M. B. Taylor, "Is dark silicon useful? Harnessing the four horsemen of the coming dark silicon apocalypse," in *Design Automation Conference (DAC), 2012 49th ACM/EDAC/IEEE*, pp. 1131–1136, June 2012.
- [54] G. V. Inc., "Neuromorphic mmory chip for pattern learning and recognition." http://general-vision.com/publications/PR_CM1KPresentation.pdf. Accessed March 25, 2016.
- [55] R. Balasubramonian, J. Chang, T. Manning, J. H. Moreno, R. Murphy, R. Nair, and S. Swanson, "Near-Data Processing: Insights from a MICRO-46 Workshop," *Micro, IEEE*, vol. 34, pp. 36–42, July 2014.
- [56] J. D. Roberts, "PROXIMITY CONTENT-ADDRESSABLE MEMORY: AN EFFICIENT EXTENSION TO k-NEAREST NEIGHBORS SEARCH (M.S. Thesis)," tech. rep., Santa Cruz, CA, USA, 1990.
- [57] A. Lipman and W. Yang, "The Smart Access Memory: An Intelligent RAM for Nearest Neighbor Database Searching," in *In ISCA Workshop on Mixing Logic and DRAM*, 1997.
- [58] T. Kohonen, *Self-organization and Associative Memory: 3rd Edition*. New York, NY, USA: Springer-Verlag New York, Inc., 1989.
- [59] P. Kanerva, *Sparse Distributed Memory*. Cambridge, MA, USA: MIT Press, 1988.
- [60] R. Shinde, A. Goel, P. Gupta, and D. Dutta, "Similarity search and locality sensitive hashing using ternary content addressable memories," in *Proceedings of the 2010 ACM SIGMOD International Conference on Management of Data*, SIGMOD '10, (New York, NY, USA), pp. 375–386, ACM, 2010.
- [61] A. Bremner-Barr, Y. Harchol, D. Hay, and Y. Hel-Or, "Ultra-fast similarity search using ternary content addressable memory," in *Proceedings of the 11th International Workshop on Data Management on New Hardware*, DaMoN'15, (New York, NY, USA), pp. 12:1–12:10, ACM, 2015.
- [62] Q. Guo, X. Guo, Y. Bai, and E. İpek, "A resistive team accelerator for data-intensive computing," in *Proceedings of the 44th Annual IEEE/ACM International Symposium on Microarchitecture*, MICRO-44, (New York, NY, USA), pp. 339–350, ACM, 2011.
- [63] Q. Guo, X. Guo, R. Patel, E. İpek, and E. G. Friedman, "Ac-dimm: Associative computing with stt-mram," *SIGARCH Comput. Archit. News*, vol. 41, pp. 189–200, June 2013.
- [64] D. Patterson, T. Anderson, N. Cardwell, R. Fromm, K. Keeton, C. Kozyrakis, R. Thomas, and K. Yelick, "A case for intelligent ram," *IEEE Micro*, vol. 17, pp. 34–44, Mar. 1997.
- [65] P. M. Kogge, T. Sunaga, H. Miyataka, K. Kitamura, and E. Retter, "Combined DRAM and logic chip for massively parallel systems," in *16th Conference on Advanced Research in VLSI (ARVLSI '95), March 27-29, 1995, Chapel Hill, North Carolina, USA*, pp. 4–16, 1995.
- [66] M. F. Deering, S. A. Schlapp, and M. G. Lavelle, "Fbram: A new form of memory optimized for 3d graphics," in *Proceedings of the 21st Annual Conference on Computer Graphics and Interactive Techniques*, SIGGRAPH '94, (New York, NY, USA), pp. 167–174, ACM, 1994.
- [67] D. Elliott, M. Stumm, W. M. Snelgrove, C. Cocjocar, and R. McKenzie, "Computational ram: Implementing processors in memory," *IEEE Des. Test*, vol. 16, pp. 32–41, Jan. 1999.
- [68] S. R. Agrawal, C. M. Dee, and A. R. Lebeck, "Exploiting Accelerators for Efficient High Dimensional Similarity Search," in *Proceedings of the 21st ACM SIGPLAN*

Symposium on Principles and Practice of Parallel Programming, PPOP '16, (New York, NY, USA), pp. 3:1–3:12, ACM, 2016.

- [69] C. D. Yu, J. Huang, W. Austin, B. Xiao, and G. Biros, “Performance Optimization for the K-nearest Neighbors Kernel on x86 Architectures,” in *Proceedings of the International Conference for High Performance Computing, Networking, Storage and Analysis*, SC '15, (New York, NY, USA), pp. 7:1–7:12, ACM, 2015.
- [70] Joint Electron Devices Engineering Council, “JESD235: High Bandwidth Memory (HBM) DRAM.” <http://www.jedec.org/standards-documents/docs/jesd235>.